Cancer Cell
Article

Oncogenic Kras-Induced GM-CSF Production Promotes the Development of Pancreatic Neoplasia

Yuliya Pylayeva-Gupta,[1] Kyoung Eun Lee,[1,4] Cristina H. Hajdu,[2] George Miller,[3] and Dafna Bar-Sagi[1,*]
[1]Department of Biochemistry and Molecular Pharmacology
[2]Department of Pathology
[3]Departments of Surgery and Cell Biology
New York University School of Medicine, New York, NY 10016, USA
[4]Present address: Abramson Family Cancer Research Institute, Howard Hughes Medical Institute, Perelman School of Medicine, University of Pennsylvania, Philadelphia, PA 19104, USA
*Correspondence: dafna.bar-sagi@med.nyu.edu
DOI 10.1016/j.ccr.2012.04.024

SUMMARY

Stromal responses elicited by early stage neoplastic lesions can promote tumor growth. However, the molecular mechanisms that underlie the early recruitment of stromal cells to sites of neoplasia remain poorly understood. Here, we demonstrate an oncogenic $Kras^{G12D}$-dependent upregulation of GM-CSF in mouse pancreatic ductal epithelial cells (PDECs). An enhanced GM-CSF production is also observed in human PanIN lesions. $Kras^{G12D}$-dependent production of GM-CSF in vivo is required for the recruitment of $Gr1^+CD11b^+$ myeloid cells. The suppression of GM-CSF production inhibits the in vivo growth of $Kras^{G12D}$-PDECs, and, consistent with the role of GM-CSF in $Gr1^+CD11b^+$ mobilization, this effect is mediated by $CD8^+$ T cells. These results identify a pathway that links oncogenic activation to the evasion of antitumor immunity.

INTRODUCTION

Pancreatic ductal adenocarcinoma (PDA) is a highly aggressive malignancy with a dismal long-term prognosis. Indeed, the disease exhibits a median survival of less than 6 months and a 5-year survival rate of 3%–5% (Kern et al., 2011; Maitra and Hruban, 2008). PDA evolves through a series of histopathological changes, referred to as pancreatic intraepithelial neoplasia (PanIN), accompanied by a recurrent pattern of genetic lesions, the earliest and most ubiquitous of which is oncogenic activation of Kras (Hong et al., 2011; Maitra and Hruban, 2008; Shi et al., 2008). The essential role of oncogenic Kras in the pathogenesis of PDA is indicated by several genetically engineered mouse models, wherein the conditional expression of the mutated allele of *Kras* in the pancreas is necessary and/or sufficient to drive disease progression from the early preinvasive to a malignant stage (Hingorani et al., 2003; Seidler et al., 2008). Though the mechanisms by which oncogenic Kras contributes to the genesis and progression of PDA have not been fully elucidated, the proliferative and survival advantages conferred on epithelial cells by the expression of endogenous oncogenic Kras have been clearly implicated (Pylayeva-Gupta et al., 2011).

In addition to the well-documented molecular and histological alterations exhibited by the tumor cells themselves, as well as by their preneoplastic precursors, a hallmark of PDA is an extensive stromal remodeling, the most prominent features of which are the recruitment of inflammatory and mesenchymal cells as well as fibrotic replacement of the pancreatic parenchyma (Chu et al., 2007; Kleeff et al., 2007; Maitra and Hruban, 2008). Strikingly, histological assessment of pancreata of human patients afflicted with PDA or mice engineered to express oncogenic Kras in the epithelial compartment of the pancreas reveals that even early stages of PanIN development are associated with a stromal reaction, which is characterized by a robust desmoplastic response and recruitment of immune cells (Chu et al.,

Significance

Pancreatic ductal adenocarcinoma (PDA) is a highly aggressive malignancy currently ranked as the fourth-leading cause of cancer-related deaths in the United States. PDA development is accompanied by pronounced changes in stromal responses and immune surveillance programs. However, the mechanisms that contribute to these changes have not been clearly defined. In this study, we demonstrate that mutational activation of Kras in pancreatic ductal cells triggers the production of GM-CSF, which, in turn, promotes the expansion of immunosuppressive $Gr1^+CD11b^+$ myeloid cells, leading to the evasion of $CD8^+$ T cell-driven antitumor immunity. Our findings implicate oncogenic Kras in restraining the antitumor immune response and provide insights into critical barriers for designing effective immunotherapeutic strategies against pancreatic cancer.

2007; Clark et al., 2007). However, the precise role played by the PanIN-associated stroma in PDA development has not been established. On the basis of the composition of the immune infiltrates surrounding the PanINs, it has been proposed that the stromal constituents around PanINs form an inflammatory and immune suppressive environment, thereby allowing the precursor lesions to escape immune surveillance (Clark et al., 2009). Consistent with this idea, studies in both humans and mice have demonstrated a dampened adaptive immune response accompanying the formation of oncogenic Ras-driven cancers (Clark et al., 2009; DuPage et al., 2011; Fossum et al., 1995; Gjertsen and Gaudernack, 1998; Kubuschok et al., 2006; Qin et al., 1995; Weijzen et al., 1999). Moreover, there is growing evidence that targeting the tumor immune microenvironment may provide an effective therapeutic strategy (Quezada et al., 2011).

To explore the functional interactions between PanINs and their microenvironment, we sought to identify the mechanisms by which precursor lesions harboring oncogenic Kras instigate a stromal response.

RESULTS

To investigate the role of oncogenic Kras in modulating the host immune response during PanIN evolution, we established an orthotopic allograft system in which primary ductal epithelial cells (PDECs) isolated from *LSL-Kras^{G12D}* knock-in mice were injected into the pancreata of syngeneic C57Bl/6 mice. The expression of the *Kras^{G12D}* allele in these cells was induced prior to implantation by Cre-mediated recombination, as previously described (Lee and Bar-Sagi, 2010); for the purpose of their in situ identification, the cells were engineered to express green fluorescent protein (GFP). Unless otherwise specified, these cells are referred to throughout the article as *GFP-Kras^{G12D}*-PDECs. To minimize the possibility of a genetic drift, PDECs were propagated in culture only for a limited number of passages (<16). As illustrated in Figure 1A, implanted *GFP-Kras^{G12D}*-PDECs formed ductal structures of heterogeneous size and architecture mostly resembling early PanIN lesions and reactive ducts. Notably, the grafts were characterized by a pronounced localized desmoplasia (Trichrome staining, Figure 1A) and the overt presence of CD45$^+$ immune cells (Figure 1B). The same results were obtained using five independent PDEC isolates, indicating that *GFP-Kras^{G12D}*-PDEC implants possess an intrinsic capacity to invoke a robust stromal response. Sham injections had no apparent effect on the pancreatic parenchyma (data not shown), ruling out the contribution of injury-induced inflammation to the observed immune response. GFP-labeled wild-type PDECs (*GFP*-WT-PDECs) failed to engraft (Figure S1A available online) consistent with their previously reported survival disadvantage relative to *Kras^{G12D}*-PDEC (Lee and Bar-Sagi, 2010).

To ascertain whether the immunologic reaction evoked by *Kras^{G12D}*-PDECs in the orthogenic system is physiologically relevant, we compared by flow cytometry analysis the overall abundance and subtype distribution of immune cells in pancreata containing *GFP-Kras^{G12D}*-PDEC grafts and pancreata from *p48-Cre;LSL-Kras^{G12D}* mice (Hingorani et al., 2003). At 8 weeks after implantation, the abundance of CD45$^+$ cells in *GFP-Kras^{G12D}*-PDEC pancreata was similar to that observed in pancreata from 12-week-old *p48-Cre;LSL-Kras^{G12D}* mice (Figure S1B), which, at this stage, typically display early PanIN lesions that are scattered throughout the organ (Hingorani et al., 2003). By and large, the distribution of the major immune cell subtypes was similar in both models (Figure 1C). In addition, both models displayed an increased intrapancreatic as well as splenic accumulation of Gr1$^+$CD11b$^+$ myeloid cells and CD4$^+$Foxp3$^+$CD25$^+$ regulatory T cells (Tregs), compared with normal pancreas and spleen (Figure 1D and Figures S1C and S1D) and in agreement with the reported increase in the abundance of these putative immunosuppressive cell populations during early pancreatic neoplasia (Clark et al., 2007). Together, these observations credential the use of *Kras^{G12D}*-PDECs to elucidate the interaction of the neoplastic epithelium with the host immune system and suggest that oncogenic activation of Kras may be sufficient to instigate immune responses that contribute to disease progression.

To further test this idea, we sought to identify mechanisms by which the expression of oncogenic Kras in PDECs could modulate an immune reaction. Given the documented effect of oncogenic forms of Ras on the expression of immune mediators (Ancrile et al., 2008; Coppé et al., 2008), we began by analyzing the supernatants of wild-type and *GFP-Kras^{G12D}*-PDECs for cytokine production using the Milliplex cytokine bead panel (Figure 2A and Figure S2A). Of the 32 cytokines represented in this panel, GM-CSF was most robustly upregulated in *GFP-Kras^{G12D}*-PDECs (Figure 2A and Figure S2A). The increase in GM-CSF protein levels was corroborated by an increase in the levels of *GM-CSF* transcripts, suggesting a role for Kras^{G12D} in the transcriptional upregulation of *GM-CSF* (Figure 2A). Pharmacological inhibition of either PI-3K or MAPK pathways resulted in abrogation of *GM-CSF* expression in *GFP-Kras^{G12D}*-PDECs, indicating that the regulation of GM-CSF expression by oncogenic Kras is mediated by multiple effector pathways (Figure 2B and Figure S2B).

To examine whether increased GM-CSF expression is also a feature of pancreatic neoplasia in vivo, we first used ELISA analysis of tissue supernatants to measure the production of GM-CSF in *GFP-Kras^{G12D}*-PDEC and *p48-Cre;LSL-Kras^{G12D}* pancreata in comparison to that from normal pancreatic tissues. In both model systems, GM-CSF levels were found to be significantly upregulated (Figure 2C). Next, we evaluated the production of GM-CSF in human PDA by immunohistochemical staining of tissue sections. At least 75% of all PanINs within a section had to exhibit 50% or more GM-CSF-stained cells per lesion to be considered positive. Using this criterion, 14 of the 16 PDA patient samples were positive for GM-CSF staining of PanIN lesions (Figure 2D). Invasive PDA lesions were also positive for GM-CSF expression, indicating that GM-CSF upregulation persists through disease progression (Figure 2D). Of note, compared to PDA-associated PanIN lesions, pancreatic lesions from four non-PDA cases (chronic pancreatitis, pancreatic dermoid cyst, pancreatic endocrine neoplasm, and serous cystadenoma) had no detectable GM-CSF expression (Figure S2C and data not shown). Because these diseases typically are not associated with mutations in the *Kras* allele, the absence of GM-CSF expression is consistent with a role for oncogenic Kras signaling in GM-CSF

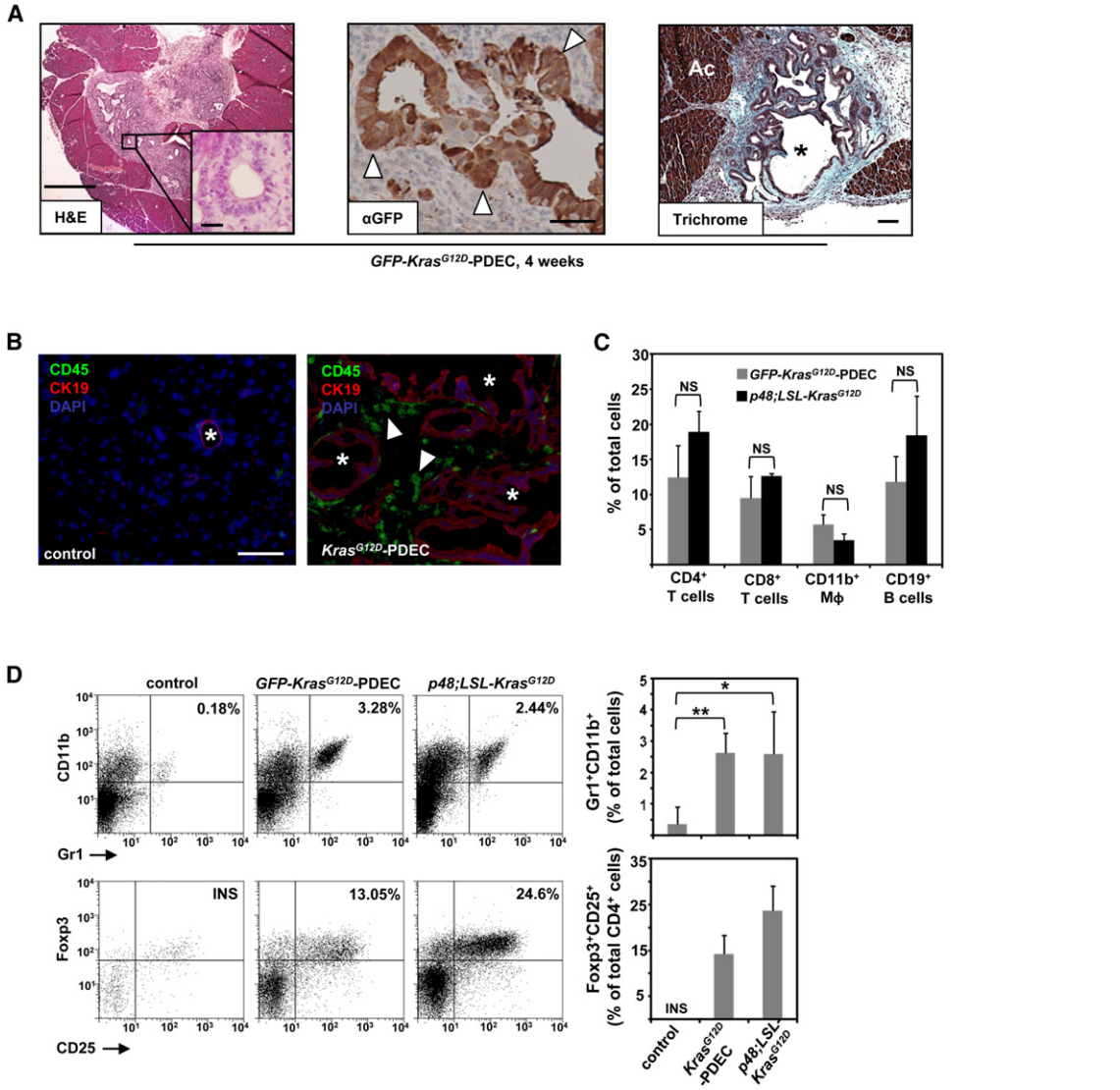

Figure 1. Orthotopic Implantation of *Kras^{G12D}*-PDECs Generates a Robust Immune Response

(A) Sections from orthotopic pancreatic grafts formed by *GFP-Kras^{G12D}*-PDECs at 4 weeks after implantation were stained with hematoxylin and eosin (H&E; scale bar, 500 μm; inset scale bar, 25 μm), anti-GFP antibody (scale bar, 50 μm), and Trichrome blue (scale bar, 100 μm). White arrowheads indicate GFP-positive neoplastic pancreatic ducts; black asterisk indicates neoplastic ducts; Ac stands for acinar compartment.

(B) Immunofluorescence staining for CD45 and CK19 in pancreata of normal sham-injected control and orthotopic *GFP-Kras^{G12D}*-PDEC animals (4 weeks after implantation). CK19 was used to identify ductal epithelia, CD45 was used to identify immune cells, and nuclei were counterstained with DAPI. White asterisk indicates pancreatic ductal structures (left panel) and grafted ductal structures (right panel); white arrowheads indicate CD45$^+$ cells. Scale bar, 100 μm.

(C) Percentage of immune cell types in pancreata was determined by flow cytometry of pancreatic tissue and quantified. After gating on the CD45$^+$ population, cells were analyzed for the presence of respective lineage markers (percentage of each immune cell subtype out of total number of live cells sorted from the pancreas is shown). Error bars indicate SD (n = 3–8 mice per group).

(D) Flow cytometry analysis of pancreatic tissue for the presence of Gr1$^+$CD11b$^+$ myeloid and Foxp3$^+$CD25$^+$ Tregs. After gating on the CD45$^+$ population (top), cells were analyzed for the presence of Gr1$^+$CD11b$^+$ subpopulation. The graph shows the percentage of Gr1$^+$CD11b$^+$ cells out of the total number of live cells sorted from the pancreas. After gating on CD45$^+$CD3$^+$ T cells (bottom), cells were gated on CD4$^+$ to examine intracellular Foxp3 versus surface CD25 staining. The graph shows the percentage of Tregs out of the total number of CD4$^+$ T cells. Representative flow cytometry plots are shown. Error bars indicate SD; INS, insufficient number of cells for analysis (n = 4–8 mice per group).

*p < 0.05; **p < 0.01; NS, not significant. See also Figure S1.

upregulation. Together, these results suggest that heightened tumor cell-derived GM-CSF levels represent an early Kras^{G12D}-dependent facet of pancreatic neoplasia that is sustained over the course of malignant transformation.

GM-CSF plays a versatile role in the development of immunological responses and has been implicated in the regulation of proliferation and maturation of multiple immune cell lineages, including monocyte, granulocyte, dendritic cells, and putative

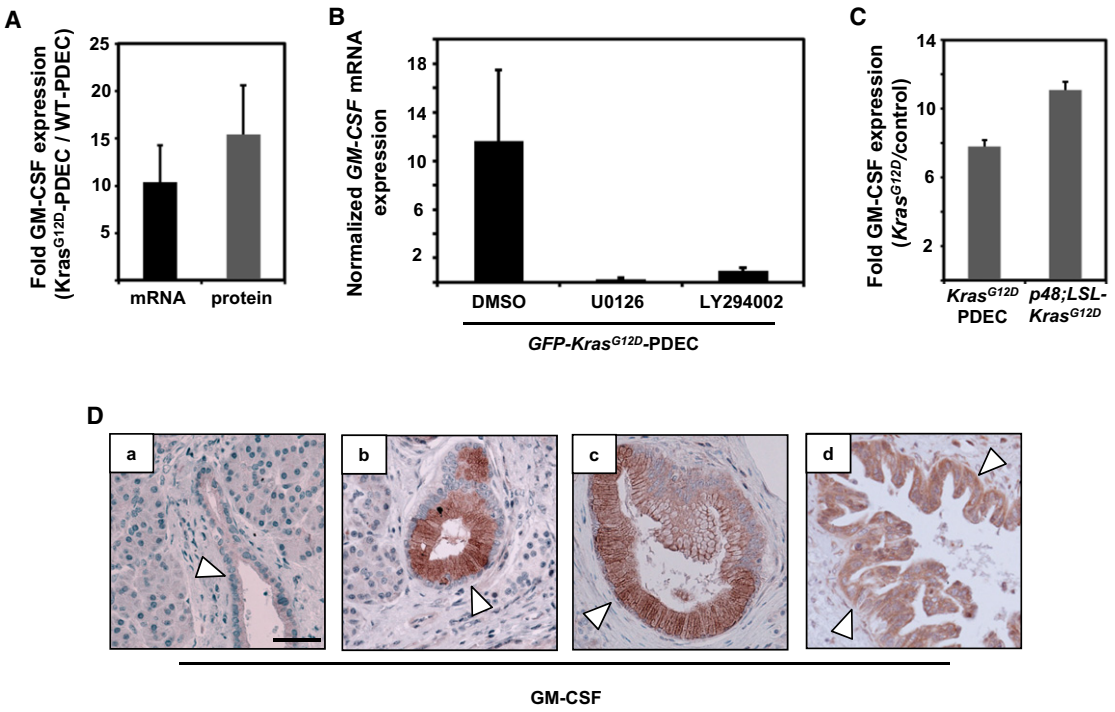

Figure 2. GM-CSF Is Upregulated in *Kras^{G12D}*-PDECs as Well as PanIN-Harboring Mouse and Human Pancreata

(A) Levels of *GM-CSF* mRNA (black bar) and protein (gray bar) in *GFP-Kras^{G12D}*-PDEC were assessed by quantitative RT-PCR and ELISA, respectively. Data are presented as an average fold induction over values from isogenic *GFP*-WT-PDECs. Error bars indicate SD (n = 3).

(B) Normalized expression of *GM-CSF* mRNA in *GFP-Kras^{G12D}*-PDECs (black bars) after 24 hr of treatment with DMSO, MAPK inhibitor U0126 (2 μM), or PI3K inhibitor LY294002 (10 μM) was analyzed by quantitative RT-PCR. Error bars indicate SD (n = 3).

(C) Levels of GM-CSF protein in pancreata grafted with *GFP-Kras^{G12D}*-PDECs or pancreata from *p48;LSL-Kras^{G12D}* mice. Data are presented as an average fold induction over values from normal pancreatic tissue. Error bars indicate SD (n = 3).

(D) Immunohistochemical staining for GM-CSF protein in representative samples of human pancreatic cancer containing PanIN lesions (a, normal duct from adjacent nonmalignant tissue; b and c, PanIN lesions; d, invasive PDA). White arrowheads indicate pancreatic duct (a), PanIN (b and c), and PDA (d). Scale bar, 50 μm.

See also Figure S2.

immunosuppressive Gr1$^+$CD11b$^+$ myeloid cells (Barreda et al., 2004). Because Gr1$^+$CD11b$^+$ cell accumulation is consistently observed in *GFP-Kras^{G12D}*-PDEC and *p48-Cre;LSL-Kras^{G12D}* pancreata (Figure 1D), we sought to determine whether the GM-CSF produced by *GFP-Kras^{G12D}*-PDEC can induce the differentiation of progenitor Gr1$^-$CD11b$^-$ cells to Gr1$^+$CD11b$^+$. As illustrated in Figure 3A, the coculturing of bone marrow-derived Lin^{neg}CD34$^+$ hematopoietic progenitor cells (HPCs) with *GFP-Kras^{G12D}*-PDECs that were seeded on Transwell inserts, induced an accumulation of Gr1$^+$CD11b$^+$ cells. Recombinant GM-CSF alone was used as a positive control (Figure 3A). The addition of neutralizing anti-GM-CSF monoclonal antibody MP1-22E9 (α-GM) (Schön et al., 2000) significantly attenuated the expansion of Gr1$^+$CD11b$^+$ cells, indicating that their generation is largely dependent on *GFP-Kras^{G12D}*-PDEC-derived GM-CSF (Figure 3A). To establish whether these Gr1$^+$CD11b$^+$ cells display suppressive activity, the coculture-derived, sorted, double-positive population was incubated with splenic T cells, and the CD3/CD28-induced proliferation of CD3$^+$ T cells was assessed by BrdU incorporation. Proliferation of CD3$^+$ cells was inhibited in the presence of Gr1$^+$CD11b$^+$ cells, indicating that GM-CSF produced by *Kras^{G12D}*-PDEC can drive the generation of differentiated Gr1$^+$CD11b$^+$ myeloid cells with immunosuppressive potential (Figure 3B). Significantly, Gr1$^+$CD11b$^+$ double-positive cells but not Gr1$^-$CD11b$^+$ single-positive cells isolated from *GFP-Kras^{G12D}*-PDEC grafted pancreata suppressed proliferation of splenic T cells (Figure 3C), indicating that the accumulation of Gr1$^+$CD11b$^+$ cells at the sites of pancreatic neoplasia could contribute to the induction of a tolerogenic immune state. Because we have observed that the numbers of Gr1$^+$CD11b$^+$ cells were augmented in the spleens of orthotopically injected animals, we sought to determine whether there was a systemic increase in the levels of GM-CSF following engraftment of *GFP-Kras^{G12D}*-PDECs. We found that the levels of circulating GM-CSF in mice with *GFP-Kras^{G12D}*-PDEC lesions were significantly elevated as compared to control animals (Figure 3D), suggesting that, in addition to its localized intrapancreatic effect, GM-CSF production by *Kras^{G12D}*-PDECs may affect hematopoietic processes in secondary lymphoid organs.

To establish whether the upregulation of GM-CSF in *Kras^{G12D}*-PDECs is responsible for the accumulation of Gr1$^+$CD11b$^+$ in vivo, we utilized short hairpin RNAi to stably knock down GM-CSF expression in *GFP-Kras^{G12D}*-PDECs. A significant

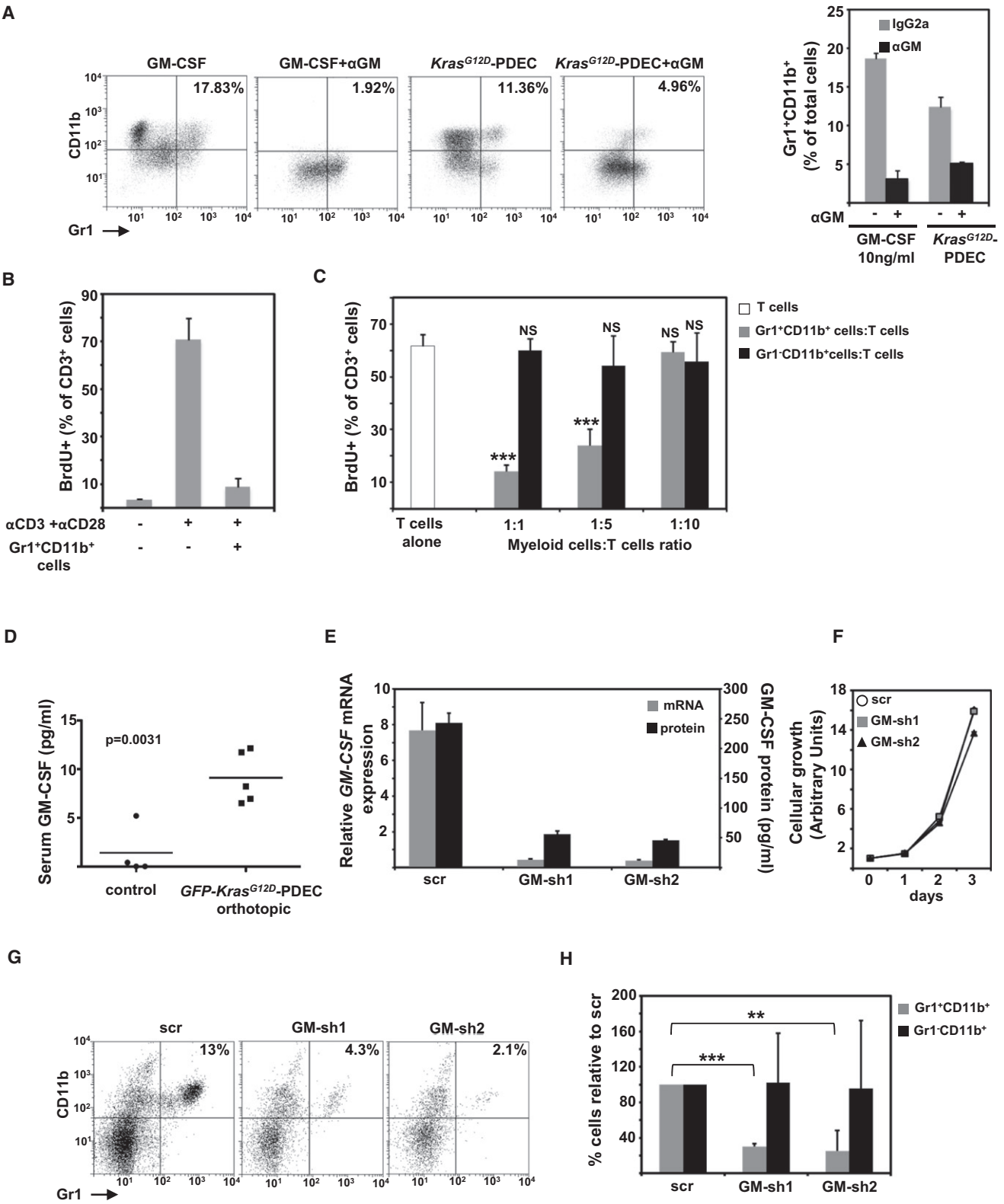

Figure 3. Kras^{G12D}-PDECs Promote Accumulation of Immunosuppressive Gr1$^+$CD11b$^+$ Cells in a GM-CSF-Dependent Manner

(A) Flow cytometry analysis of Lin^{neg}CD34$^+$ hematopoietic progenitor cells for the surface markers CD11b and Gr1 following coculture with GM-CSF or *GFP-Kras^{G12D}*-PDECs with or without α-GM-CSF antibody (α-GM). Representative flow cytometry plots and a graph indicating percentage of the Gr1$^+$CD11b$^+$ cells out of the total number of live cells are shown. Error bars indicate SD (n = 3).

reduction of GM-CSF at the level of both mRNA and protein was achieved using two independent hairpin sequences (Figure 3E). GM-CSF knock-down did not produce an adverse effect on the growth of *GFP-Kras^{G12D}*-PDEC in culture (Figure 3F), consistent with our findings that these cells do not express the GM-CSF receptor beta chain CD131 (data not shown). We next analyzed the composition of leukocytic infiltrates in pancreata grafted with *GFP-Kras^{G12D}*-PDECs expressing scrambled (scr-*GFP-Kras^{G12D}*-PDEC) or GM-CSF shRNAs (GM-sh1- and GM-sh2-*GFP-Kras^{G12D}*-PDEC). Among all $CD45^+$ cells found in the pancreas, GM-CSF knock-down led to a specific reduction in the abundance of $Gr1^+CD11b^+$ cells but not $Gr1^-CD11b^+$ cells (Figures 3G and 3H), indicating that the production of GM-CSF by ductal cells harboring the *Kras^{G12D}* allele is necessary to promote local accumulation of immune cells of the $Gr1^+CD11b^+$ lineage.

Because $Gr1^+CD11b^+$ myeloid cells have been implicated in tumor-induced immune tolerance (Gabrilovich and Nagaraj, 2009), we reasoned that the *Kras^{G12D}*-PDEC-mediated production of GM-CSF and the resulting accumulation of $Gr1^+CD11b^+$ cells could be critical for the establishment of an immunosuppressive environment that is growth permissive. To investigate this possibility, we have characterized the engraftment of *GFP-Kras^{G12D}*-PDEC in relation to GM-CSF production. As illustrated in Figure 4A, the implantation frequency of GM-sh-*GFP-Kras^{G12D}*-PDECs was significantly reduced as compared to scr-*GFP-Kras^{G12D}*-PDECs, and the average size of the knock-down lesions was significantly decreased. To gain insight into the process underlying compromised engraftment of GM-sh-*GFP-Kras^{G12D}*-PDECs, we analyzed the fate of the grafts at different time points after implantation by immunohistochemical staining against GFP. At 1 week after implantation, grafts generated from scr- and GM-sh-*GFP-Kras^{G12D}*-PDECs were essentially indistinguishable with respect to size, histological appearance, and cell number (Figure 4B and Figure S3). Thus, it appears that GM-CSF deficiency has no adverse effect on the initial growth and survival capabilities of *Kras^{G12D}*-PDEC in vivo. However, at 2 weeks after implantation, although scr-*GFP-Kras^{G12D}*-PDEC grafts displayed a sizable expansion and the characteristic elaboration of ductal structures, graft areas in pancreata that were implanted with GM-sh-*GFP-Kras^{G12D}*-PDECs were virtually devoid of GFP-positive cells (Figure 4B and Figure S3). These observations are consistent with the postulate that the production of GM-CSF enables *Kras^{G12D}*-PDEC to engage host-dependent responses that favor their maintenance and expansion.

Recent studies have indicated that $Gr1^+CD11b^+$ cells may contribute to tumor immune evasion by restraining the activity of $CD8^+$ T cells (Gabrilovich and Nagaraj, 2009; Marigo et al., 2008). To examine the relevance of this mechanism to the engraftment potential of *Kras^{G12D}*-PDECs, the accumulation of $CD8^+$ T cells was analyzed by immunohistochemistry. The pancreatic parenchyma associated with grafts from scr-*GFP-Kras^{G12D}*-PDECs was devoid of $CD8^+$ T cells both at 1 and 2 weeks after implantation (Figure 5A and Figure S4A). In contrast, a pronounced accumulation of $CD8^+$ T cells in the parenchyma of GM-sh-*GFP-Kras^{G12D}*-PDEC grafts was detected at 2 weeks after implantation (Figure 5A). A similar pattern of $CD8^+$ cell accumulation was observed when control or GM-sh-*Kras^{G12D}*-PDEC lacking GFP expression were injected into the pancreas, indicating that the $CD8^+$ T cell response was not instigated by ectopically expressed GFP, but was elicited by the transformed epithelium (Figure S4B). Significantly no infiltration of $CD8^+$ cells was observed at 1 week after implantation in GM-sh-*GFP-Kras^{G12D}*-PDEC grafts (Figure S4A), consistent with the time requirement associated with the priming of the adaptive immune responses. Of note, at later time points after implantation (~4 weeks), some of the $CD8^+$ T cells were found in clusters that contain B cells, likely signifying the formation of secondary lymphoid tissue, which is indicative of a persisting immune response (Carragher et al., 2008) (Figure 5B).

Coincident with the accumulation of $CD8^+$ T cells, we have observed an increase in the frequency of apoptosis within the GM-CSF knock-down grafts only at 2 weeks after implantation (Figure 5A and Figure S4A). These results suggest that, in the absence of GM-CSF, the cytotoxic activity of $CD8^+$ T cells at the site of engraftment may be responsible for the clearance of implanted *GFP-Kras^{G12D}*-PDECs. A prediction borne by this interpretation is that the growth defect of GM-sh *Kras^{G12D}*-PDECs would be rescued by $CD8^+$ T cell depletion. To test this prediction, we performed orthotopic implantations in animals depleted of $CD8^+$ T cells by intraperitoneal administration of anti-CD8 antibody over a period of 2 weeks. This regiment resulted in >90% depletion of $CD3^+CD8^+$ T cells (Figure S5). At 2 weeks after implantation, no GM-sh-*GFP-Kras^{G12D}*-PDECs were detected in pancreata animals injected with control

(B) Quantification of $BrdU^+CD3^+$ T cells treated as indicated. T cells and $Gr1^+CD11b^+$ cells were cocultured at a 1:1 ratio. Error bars indicate SD (n = 3).
(C) Representative quantification of $BrdU^+CD3^+$ T cells cocultured with either $Gr1^-CD11b^+$ or $Gr1^+CD11b^+$ cells isolated from mouse pancreata 8 weeks after injection with *GFP-Kras^{G12D}*-PDECs. For proliferation assays, myeloid cells and T cells were cultured at ratios of 1:1, 1:5, or 1:10 respectively. T cells incubated in αCD3-coated wells and in the presence of αCD28 serve as control. Error bars indicate SD (n = 3).
(D) Expression of mouse GM-CSF in the sera of either uninjected mice (control, n = 4) or mice with *GFP-Kras^{G12D}*-PDEC grafts 8 weeks after implantation (n = 5) was measured using ELISA. Each symbol represents a mouse, and mean values for each group are represented by black lines.
(E) Relative expression of *GM-CSF* mRNA (gray bars, left axis) and protein (black bars, right axis) in *GFP-Kras^{G12D}*-PDECs 4 days after infection with lentiviruses containing either scrambled shRNA (scr) or GM-CSF shRNAs (GM-sh1, GM-sh2) was assessed by quantitative RT-PCR and ELISA. Error bars indicate SD (n = 3).
(F) Growth analysis of scr (circles), GM-sh1 (squares), and GM-sh2 *GFP-Kras^{G12D}*-PDEC (triangles) was assessed by MTT assay. Error bars indicate SD (n = 3).
(G) Representative flow cytometry plots of pancreatic immune cells for the surface expression of Gr1 and CD11b markers at 4 weeks after implantation of scr-, GM-sh1-, and GM-sh2 *GFP-Kras^{G12D}*-PDEC. After gating on the $CD45^+$ population, cells were analyzed for the presence of $CD11b^+$ and $Gr1^+$ populations.
(H) Quantification of relative abundance of $Gr1^+CD11b^+$ and $Gr1^-CD11b^+$ cell populations is presented as a percentage change in $CD45^+$ single-positive $Gr1^-CD11b^+$ cells (black bars) and double-positive $Gr1^+CD11b^+$ population (gray bars) relative to scr *GFP-Kras^{G12D}*-PDECs. Error bars indicate SD (n = 6 mice per group).
$^{**}p < 0.01$; $^{***}p < 0.001$; NS, not significant.

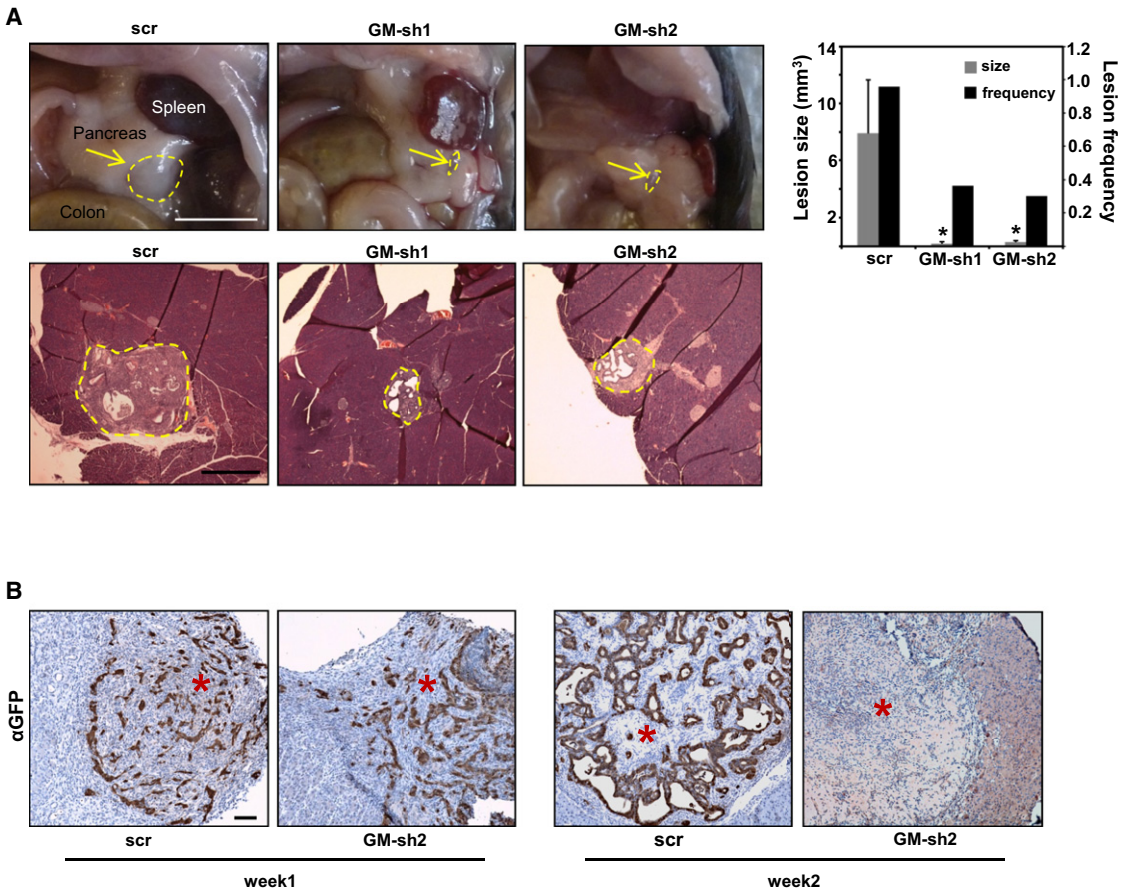

Figure 4. Functional Consequence of Ablating GM-CSF on Growth of *Kras^{G12D}*-PDECs In Vivo

(A) Gross anatomical view of scr- and GM-sh *GFP-Kras^{G12D}*-PDEC grafts (top, dotted outlines and arrows) at 8 weeks after implantation. Scale bar, 5 mm. Quantification of the graft size at 8 weeks after implantation (gray bars, left axis) and percentage of overall lesion frequency (black bars, right axis) is indicated in the graph. Error bars indicate SD (n = 3). Sections from pancreata containing scr- and GM-sh *GFP-Kras^{G12D}*-PDEC orthotopic grafts at 4 weeks after implantation were stained with H&E (bottom, lesions are delineated by dotted outlines). Scale bar, 500 μm.

(B) Immunohistochemical staining for GFP on sections of scr- and GM-sh *GFP-Kras^{G12D}*-PDEC orthotopic grafts at 1 and 2 weeks after implantation. Red asterisks indicate engrafted area. Scale bar, 100 μm.

*$p < 0.05$. See also Figure S3.

antibody (Figure 6), and the implanted area displayed many apoptotic cells (data not shown). In contrast, the injection of anti-CD8 antibody was sufficient to permit the establishment of GM-sh-*GFP-Kras^{G12D}*-PDEC grafts that were indistinguishable in size and overall appearance from scr-*GFP-Kras^{G12D}*-PDEC grafts (Figure 6), indicating that CD8$^+$ T cells are the primary immune cell type responsible for mounting and executing the immune response against *Kras^{G12D}*-PDEC.

DISCUSSION

The critical role of host immunity in regulating tumorigenesis is undisputed (Grivennikov et al., 2010). Furthermore, it is becoming increasingly evident that immune cells in the tumor microenvironment fail to mount an effective antitumor immune response (Ruffell et al., 2010). However, the underlying mechanisms that allow tumors to escape immune surveillance have not been fully characterized. In the present study, we implicate oncogenic Kras in restraining the antitumor immune response through the production of GM-CSF and the subsequent suppression of T cell immunity. This immune evasion strategy may contribute to immunotherapeutic resistance in oncogenic Kras-driven cancers.

The progression of pancreatic neoplasia is accompanied by cellular and molecular alterations in both the parenchymal and stromal compartments of the pancreas (Kleeff et al., 2007). The parenchymal component gives rise to PanINs, and the contribution of oncogenic Kras to this transition has been amply documented using genetically engineered mouse models (Hingorani et al., 2003, 2005). In contrast, little is known about the stroma-modulating capabilities of oncogenic Kras during the early stages of pancreatic cancer. The demonstration that GM-CSF production in response to activation of Kras modulates the immune reaction to pancreatic precursor lesions thus provides insights into how this oncogenic event could lead to the reprogramming of the microenvironment from the very beginning of the disease. The recent demonstration of the role of pancreas-specific oncogenic activation of Kras in generating

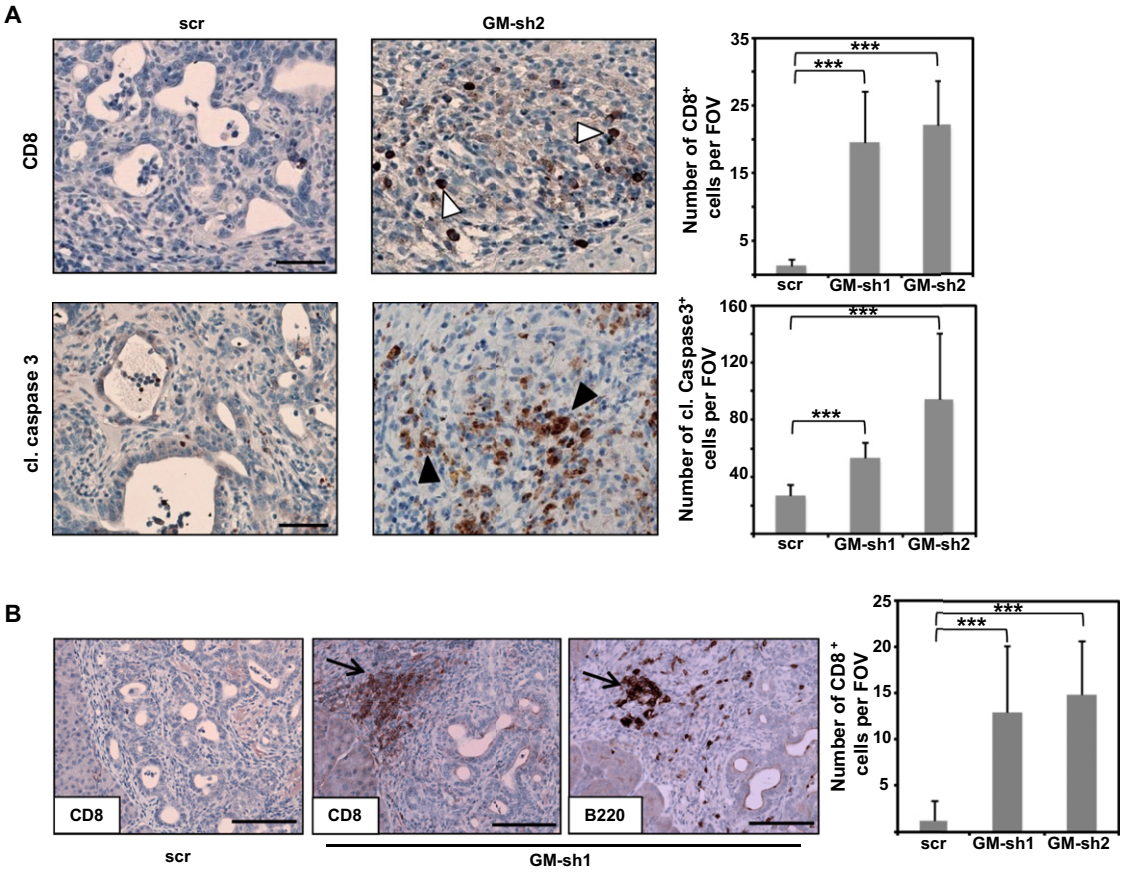

Figure 5. Engraftment of GM-CSF Knock-Down *Kras^{G12D}*-PDEC Is Accompanied by an Increase in Infiltrating CD8$^+$ T Cells

(A) Immunohistochemical staining and quantification of CD8 and cleaved caspase 3 staining on sections of scr- and GM-sh *GFP-Kras^{G12D}*-PDEC orthotopic grafts at 2 weeks after implantation. CD8$^+$ or cleaved caspase3-positive cells within the boundaries of orthotopic grafts were counted per field of view (FOV) at 20× magnification. White arrowheads indicate CD8$^+$ cells; black arrowheads indicate caspase-3-positive cells. Scale bars, 50 μm. Error bars indicate SD (n = 4 mice per group, 4 FOV per mouse).

(B) Immunohistochemical staining for CD8 and B220 on consecutive sections of scr- and GM-sh *GFP-Kras^{G12D}*-PDEC orthotopic grafts at 4 weeks after implantation. Numbers of CD8$^+$ cells were counted per FOV at 20× magnification and are shown in the graph. Arrows indicate coaggregation of CD8$^+$ cells and B220$^+$ cells. Scale bar, 100 μm. Error bars indicate SD (n = 3 mice per group, 5 FOV per mouse).

***p < 0.001. See also Figure S4.

a protumorigenic inflammatory microenvironment (Fukuda et al., 2011; Lesina et al., 2011) further underscores the crucial contribution of non-cell-autonomous mechanisms to pancreatic tumor initiation and progression.

The identification of GM-CSF as a transcriptional target of oncogenic Kras in PDECs is consistent with the existence of Ras-regulated transcription factor-binding sites, such as AP-1 and ETS, in the *GM-CSF* promoter region (Osborne et al., 1995). The pathophysiological relevance of the activation of this transcriptional program is indicated by the increased levels of GM-CSF we have observed in human PanIN lesions. It is possible that a similar Kras-mediated mechanism of GM-CSF upregulation is responsible for the enhanced serum levels of GM-CSF detected in patients with pancreatic cancer (Mroczko et al., 2005). Our initial analysis suggests that the upregulation of GM-CSF in response to oncogenic Kras is mediated by the concerted action of multiple effector pathways, including Erk and PI-3K (Figure 2B). Because these pathways are frequently activated in various malignancies, the induction of GM-CSF might not be restricted to oncogenic Kras-driven cancers and/or the pancreas. This idea is supported by studies demonstrating the overexpression of GM-CSF in several human cancer lines, including those of breast, bladder, and melanoma origin (Bronte et al., 1999; Dolcetti et al., 2010; Steube et al., 1998). Thus, the functional significance of GM-CSF upregulation might have broader implications.

Under normal physiological conditions, GM-CSF serves as a bona fide growth factor for hematopoietic cells, promoting the proliferation and maturation of multiple myeloid cell lineages in a concentration-dependent manner (Barreda et al., 2004). In neoplastic settings, GM-CSF has been shown to be endowed with the potential to exert both pro- and antitumorigenic effects by suppressing or enhancing tumor immunity, respectively (Hamilton, 2008). Our findings demonstrate that, in pancreatic ductal cells harboring oncogenic Kras, GM-CSF production is linked to the expansion of Gr1$^+$CD11b$^+$ myeloid cells. A similar consequential relationship between GM-CSF generation and Gr1$^+$CD11b$^+$ cell expansion has been documented in other

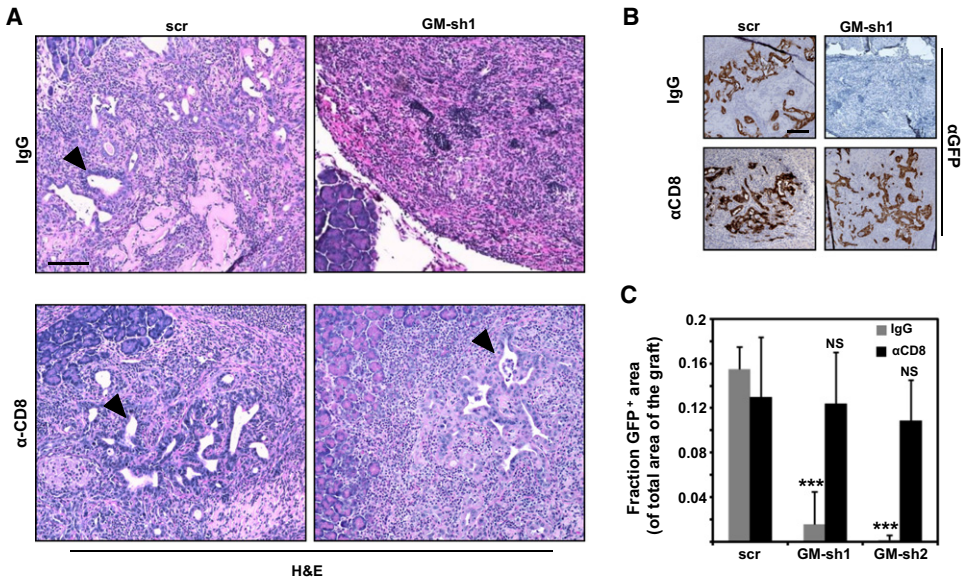

Figure 6. CD8$^+$ T Cells Are Instrumental in the Clearance of GM-CSF Knock-Down *Kras^{G12D}*-PDECs

(A) Orthotopic grafts formed by scr- or GM-sh *GFP-Kras^{G12D}*-PDECs implanted into either mock-depleted (IgG) or CD8-depleted animals were analyzed at 2 weeks after implantation by H&E. Black arrowheads indicate pancreatic ductal structures. Scale bar, 100 μm.

(B) The extent of colonization of the grafted areas by scr- or GM-sh *GFP-Kras^{G12D}*-PDECs in mock-depleted (IgG) or CD8-depleted animals at 2 weeks after implantation was analyzed by immunohistochemistry for GFP. Scale bar, 100 μm.

(C) Graph depicts quantification of the data from (B) and indicates the fraction of GFP$^+$ area per total area of the graft. Error bars indicate SD (n = 4 mice per group, 5 FOV per mouse).

***p < 0.001; NS, not significant. See also Figure S5.

tumor models (Dolcetti et al., 2010; Marigo et al., 2010; Morales et al., 2010). However, in the mouse, Gr1$^+$CD11b$^+$ double-positive cells represent a heterogeneous population composed of myeloid derived suppressor cells, monocytes, and immature myeloid cells (Ostrand-Rosenberg and Sinha, 2009). Several lines of evidence suggest that the Gr1$^+$CD11b$^+$ cells that accumulate in response to GM-CSF production by pancreatic precursor lesions are immunosuppressive in nature. First, when isolated from pancreata grafted with *GFP-Kras^{G12D}*-PDECs, the Gr1$^+$CD11b$^+$ cells displayed a suppressive effect in a T cell proliferation assay. Second, the reduction in the abundance of Gr1$^+$CD11b$^+$ cells following the suppression of GM-CSF expression in vivo was accompanied by the infiltration of CD8$^+$ T cells. Third, the immune response-mediated elimination of orthotopic *GFP-Kras^{G12D}*-PDEC lesions observed under these conditions could be fully rescued by CD8$^+$ T cell depletion, indicating a principal role for Gr1$^+$CD11b$^+$ cells in disrupting T cell immune surveillance during the early stages of pancreatic neoplasia. The potential relevance of this immune modulatory mechanism to more advanced stages of pancreatic cancer is suggested by the reciprocal relationship between CD8$^+$ T and Gr1$^+$CD11b$^+$ cell infiltrates observed in pancreatic tumors from the *p48-Cre;LSL-Kras^{G12D}* mice (Clark et al., 2007).

GM-CSF is not unique in its ability to promote the expansion and tumor mobilization of Gr1$^+$CD11b$^+$ immunosuppressive cells. For example, IL1-β, IL-6, and VEGF have been shown to induce the accumulation of Gr1$^+$CD11b$^+$ myeloid cells and the concomitant suppression of T cell immune response in a variety of mouse tumor models (Bunt et al., 2007; Melani et al., 2003; Pilon-Thomas et al., 2011; Tu et al., 2008). Significantly, IL1-β, IL-6, and VEGF are targets of oncogenic Ras signaling, and their production by cancer cells harboring oncogenic Ras has been implicated in various protumorigenic processes, such as inflammation, angiogenesis, and metastasis (Ancrile et al., 2008; Coppé et al., 2008; Kranenburg et al., 2004). Because the expression of IL1-β, IL-6, and VEGF in *GFP-Kras^{G12D}*-PDECs is not elevated relative to the levels measured in wild-type PDECs (Figure S2A) and the suppression of GM-CSF production is accompanied by a decrease in Gr1$^+$CD11b$^+$ cells, we conclude that the production of GM-CSF by the precursor lesions formed by these cells is necessary and sufficient to induce the observed increase in Gr1$^+$CD11b$^+$ cells and the impaired response of CD8$^+$ T cells. The molecular mechanisms responsible for the selective upregulation of GM-CSF observed in *Kras^{G12D}*-PDECs remain to be defined. Differences in genetic profile, cellular background, and levels of Ras expression between the experimental system described in this study and those used in other reports could be important contributors. Moreover, our findings do not rule out the possibility that IL1-β, IL-6, and VEGF as well as potentially other secreted factors can participate in establishing an immunosuppressive environment in oncogenic Ras-driven cancers. The existence of such redundancy in the mechanism by which oncogenic Ras can invoke tumor-induced tolerance may serve to secure the sustenance of this mechanism at various stages of tumor development.

Our studies reinforce the role of intrinsic immune surveillance in restraining tumor initiation and support the idea that the

evolution of pancreatic neoplasia is critically dependent on the subversion of T cell responses against antigens that are expressed by pancreatic tumor cells. Although the specific antigen recognized by the CD8$^+$ cells in our experimental system remains to be identified, it is of relevance to note that a T cell response against oncogenic Ras has been documented in a significant proportion of patients with PDA (Gedde-Dahl et al., 1994; Kubuschok et al., 2006; Linard et al., 2002; Weijzen et al., 1999). Given the ubiquitous occurrence of oncogenic Kras mutations in pancreatic adenocarcinomas, the disruption of mechanisms that induce T cell tolerance might offer a broadly applicable strategy for the targeting of immune escape in pancreatic cancer.

EXPERIMENTAL PROCEDURES

Animal Models

The *LSL-Kras^{G12D}* and *p48-Cre* strains have been described previously (Jackson et al., 2001; Kawaguchi et al., 2002). C57BL/6 mice were obtained from The Charles River Laboratories. For orthotopic implantation of PDECs, mice were anesthetized using a ketamine/xylazine cocktail, and a small (7 mm) left abdominal side incision was made. PDECs (1 × 10^6 cells/mouse) were suspended in Matrigel (Becton Dickinson) diluted 1:1 with cold PBS (total volume of 50 μl) and were injected into the tail region of the pancreas using a 26-gauge needle. A successful injection was verified by the appearance of a fluid bubble without intraperitoneal leakage. The abdominal wall was closed with absorbable Vicryl *RAPIDE* sutures (Ethicon), and the skin was closed with wound clips (Roboz). Mice were sacrificed at the indicated time points, and grafts were measured and processed for histology or flow cytometry. All animal care and procedures were approved by the Institutional Animal Care and Use Committee at NYU School of Medicine.

Isolation, Culture, and Infection of PDECs

Isolation, culture, and adenoviral infection of PDECs were performed as previously described (Agbunag et al., 2006; Lee and Bar-Sagi, 2010). Lentiviral vectors containing shRNAs directed against the *GM-CSF* gene (GM-sh1 and GM-sh2; clone ID TRCN0000054618 and TRCN0000054620) and control scrambled shRNA (scr) were obtained from Open Biosystems (pLKO.1, TRC Consortium). Lentiviral vector encoding GFP (pLVTHM-GFP) was a kind gift from Dr. F. Giancotti. To generate lentiviral particles, HEK293T cells were cotransfected with the vector, the packaging construct (pHR-CMV-dR8.2), and the envelope plasmid (pCMV-VSVG). Viral stocks were collected for 2 days, filtered through a 0.45 μm filter, and concentrated using 100MWCO Amicon Ultra centrifugal filters (Millipore). A multiplicity of infection of 15 was used for lentiviral infection of WT- or *Kras^{G12D}*-PDECs in the presence of 10 μg/ml Polybrene (Chemicon).

Immunoblot Analysis

Cells were lysed in 1% Triton-X buffer (50 mM HEPES [pH 7.4], 1% Triton X-100, 150 mM NaCl, 10% glycerol, 1 mM EGTA, 1 mM EDTA, 25 mM NaF, 1 mM Na vanadate, 1 mM phenylmethanesulfonyl fluoride [PMSF] and protease inhibitors). The following primary antibodies were used: mouse anti-HA (12CA5), mouse anti-vinculin (Sigma-Aldrich), rabbit anti-phospho-ERK (Cell Signaling), mouse anti-ERK (Cell Signaling), rabbit anti-phospho-AKT (S473, Cell Signaling), and rabbit anti-AKT (Cell Signaling). After incubation with either the secondary IRDye Alexa Fluor 680 goat anti-mouse antibody or 800 goat anti-rabbit antibody (Molecular Probes), the membranes were visualized with the Odyssey Infrared Imaging System (Li-Cor).

Quantitative RT-PCR

Extraction and reverse transcription of total RNA from PDECs was performed using RNeasy mini kit (QIAGEN) and QuantiTect reverse transcription kit (QIAGEN), respectively. SYBR Green PCR Master Mix (USB) was used for amplification, and the samples were run on the Stratagene Mx 3005P. Expression levels were normalized by GAPDH.

Human Pancreas Specimens

The use of human tissue was reviewed and approved by the Institutional Review Board of NYU School of Medicine, and samples (provided by the Tissue Acquisition and Biorepository Service) were obtained after informed consent. Sections (5 μm) were cut from formalin-fixed paraffin-embedded samples for the purpose of immunohistochemistry. A total of 16 pancreatic adenocarcinoma, one chronic pancreatitis, one benign pancreatic cyst, one serous cystadenoma, and one intraductal papillary mucinous neoplasm samples were analyzed.

Histology and Immunohistochemistry

Mouse pancreata were fixed overnight in 10% formalin (Fisher) and were processed for paraffin embedding. For histology, deparaffinized sections (6 μm) were stained with Harris hematoxylin and eosin (both from Sigma-Aldrich) followed by an alcohol dehydration series and mounting (Permount, Fisher). Trichrome staining was performed at NYU School of Medicine Histopathology Core Facility. For immunohistochemistry, deparaffinized sections (6 μm) were rehydrated and quenched in 1% hydrogen peroxide/methanol for 15 min, and antigen retrieval was performed in 10 mM sodium citrate and 0.05% Tween-20 (pH 6.0) for 15 min in a microwave oven. Blocking was done in 10% serum, 1% BSA, and 0.5% Tween-20 for 1 hr at room temperature, followed by incubation with the primary antibodies diluted in 2% BSA overnight at 4°C. The following primary antibodies were used: rabbit anti-GFP (Cell Signaling), rabbit anti-GM-CSF (Novus Biologicals), rat anti-CD8 (53-6.7, BD Biosciences), rabbit anti-cleaved caspase-3 (Cell Signaling), and rat anti-B220 (BD Biosciences). After incubating with secondary biotinylated antibodies and ABC solution (both from Vector Laboratories), sections were developed with 3,3′-diaminobenzidine tetrahydrochloride (Sigma-Aldrich). After counterstaining with Harris hematoxylin (Sigma), slides were subjected to an alcohol dehydration series and mounted with Permount (Fisher). Slides were examined on a Nikon Eclipse 80i microscope.

Immunofluorescence

Mouse pancreata were embedded in OCT compound (Tissue-Tek) by snap freezing OCT-covered tissues in liquid nitrogen, and 8 μm sections were cut on a Leica microtome. After fixing the sections in 4% paraformaldehyde for 10 min on ice and permeabilizing with 0.25% Triton X-100 for 10 min on ice, sections were blocked with 10% serum, 2% BSA, and 0.1% Tween-20 for 1 hr at room temperature. Incubation with primary antibodies diluted in 2% BSA and 0.5% Tween-20 was performed overnight at 4°C. The following antibodies were used: rat anti-CD45 (BD Biosciences) and rat anti-CK19 (Troma III, developed by R. Kemler, made available by Developmental Studies Hybridoma Bank under the auspices of the NICHD). After incubating with Alexa Fluor-labeled secondary antibodies (Invitrogen) diluted in 1% BSA for 1 hr at room temperature, sections were stained with DAPI and mounted using polyvinyl alcohol mounting media with DABCO (Fluka). Slides were examined on a Zeiss Axiovert 200M microscope.

Flow Cytometry

Cellular suspensions from the tissues were prepared as follows: spleens were mechanically disrupted, suspended in 1% FBS and PBS, passed through a 70 μm strainer, and treated with RBC lysis buffer (eBioscience). Pancreata were minced using sterile razor blades and were incubated in 1.25 mg/ml collagenase type IV and 0.1% soybean trypsin inhibitor (Sigma-Aldrich) in RPMI for 15 min at 37°C. Cells were suspended in 1% FBS and PBS, were passed through a 70 μm strainer, and were treated with RBC lysis buffer. Single-cell suspensions from spleens and pancreata were blocked with anti-CD16/CD32 antibody (Fc Block, BD Biosciences) for 5 min on ice and were labeled with the following antibodies: anti-CD45.2 (104), anti-CD3ε (500A2), anti-CD4 (RM4-5), anti-CD8α (53-6.7), anti-CD45R/B220 (RA3-6B2), anti-CD19 (1D3), anti-CD11b (M1/70), anti-Gr1 (RB6-8C5), and anti-CD25 (PC61.5) (all from BD Biosciences). Staining for intracellular Foxp3 was performed using Mouse Regulatory T Cell Staining Kit (FJK-16, eBioscience). Dead cells were excluded by staining with propidium iodine (Sigma-Aldrich). Flow cytometry was performed on FACScan (BD Biosciences) at NYU School of Medicine Flow Cytometry Core Facility, and data were analyzed using FlowJo software.

Supernatant Collection and Cytokine Analysis

For cytokine analysis of PDEC cultures, cells were cultured in complete medium at a concentration of 1 × 10^6 cells/ml for 24 hr before supernatant harvest. For cytokine analysis of mouse pancreata, the tissues were harvested, weighed, minced with a sterile razor blade, and incubated in 500 μl of complete media for 24 hr before supernatant collection. Analysis of the cytokines was done with Milliplex Map Immunoassay (Millipore) and the Luminex 200 system (Luminex) according to the manufacturer's instructions. Where indicated, mouse GM-CSF protein levels were determined by Mouse GM-CSF Quantikine ELISA Kit (mean MDD = 1.8 pg/ml; R&D Systems). For analysis of GM-CSF levels in mouse sera, blood samples were collected retro-orbitally, and the samples were processed according to the manufacturer of the ELISA kit.

Culture of Sorted HPCs

Bone marrow cells were isolated from C57Bl/6 mice, and HPCs were sorted using Mouse Hematopoietic Stem and Progenitor Cell Isolation Kit (BD Biosciences), according to the manufacturer's instructions. Isolated HPCs were cultured in 6-well plates (1 × 10^5 cells/well) for a total of 6 days. On day 0, either GM-CSF (10 ng/ml, Monoclonal Antibody Core Facility at Memorial Sloan-Kettering Cancer Center) or a 24 mm Transwell insert with a 0.4 μm pore size (Corning Life Sciences) containing *Kras^{G12D}*-PDEC (2 × 10^5 cells/insert) were added to the HPCs. On day 3, fresh cytokine or inserts with cells were added. Where indicated, HPC cultures were supplemented with either control IgG2a antibody (1 μg/ml, eBioscience) or anti-GM-CSF antibody (1 μg/ml MP1-22E9, eBioscience). For T cell proliferation assays, Gr1$^+$CD11b$^+$ cells were sorted on day 6 of culture. Cellular purity was greater than 90%.

Proliferation and Viability Assays

For in vitro T cell proliferation assays, splenic T cells suspended in complete RPMI medium were added to 96-well plates precoated with anti-CD3 antibody (BD Biosciences) at a density of 5 × 10^4 cells/well. Anti-CD28 antibody (37.51, eBioscience) was added to T cells at a concentration of 1 μg/ml. Autologous Gr1$^+$CD11b$^+$ cells derived from coculture of *Kras^{G12D}*-PDEC and HPC were irradiated and added in triplicates directly to T cells (5 × 10^4 Gr1$^+$CD11b$^+$ cells/well) 24 hr before adding BrdU reagent. Pancreas-associated myeloid Gr1$^-$CD11b$^+$ or Gr1$^+$CD11b$^+$ cells were sorted from *Kras^{G12D}*-PDEC-grafted pancreata at 8 weeks after implantation and were added in triplicates and at indicated ratios directly to T cells 24 hr before adding BrdU reagent (Sigma-Aldrich). T cells were labeled by adding BrdU to the culture medium at a final concentration of 10 μM for 48 hr. Staining for BrdU was achieved using APC BrdU Flow Kit (BD Biosciences). The percentage of BrdU-positive T cells was determined by FACS analysis of CD3$^+$BrdU$^+$ cells.

For *Kras^{G12D}*-PDEC growth assays, cells were seeded at a density of 2,000 cells/well in a 96-well plate. At indicated time points, cell culture medium was aspirated, the wells were washed with RPMI (without phenol red, BioWhittaker), and 0.5 mg/ml 3-[4,5-dimethylthiazol-2-yl]-2,5-diphenyl tetrazolium bromide (MTT; Sigma-Aldrich) was added for 2 hr at 37°C. The reagent was aspirated, and 100 μl of DMSO was added to each well for 20 min at room temperature. Plates were read at an absorbance of 570 nm using a VERSAmax microplate reader (Molecular Devices). For the day 0 time point, cells were treated with MTT reagent 2 hr after plating.

CD8 Depletion

Mice were depleted of CD8$^+$ T cells via intraperitoneal injection of control rat IgG antibody (eBioscience) or anti-CD8a antibody at a concentration of 0.2 mg/mouse (53-6.72, Monoclonal Antibody Core Facility at Memorial Sloan-Kettering Cancer Center). Injections were administered every day for 3 days prior to orthotopic injection, and twice a week thereafter until the experimental endpoint. The efficiency of CD8$^+$ T cell depletion was assessed by FACS of splenic tissues using anti-CD3 and anti-CD8 antibodies.

Statistical Analyses

Data are presented as means ± standard deviations (SD). Quantification of GFP positivity was performed using ImageJ analysis. Data were analyzed by the Microsoft Excel or GraphPad Prism built-in t test (unpaired, two-tailed), and results were considered significant at $p < 0.05$.

SUPPLEMENTAL INFORMATION

Supplemental Information includes five figures and can be found with this article online at doi:10.1016/j.ccr.2012.04.024.

ACKNOWLEDGMENTS

We thank L.J. Taylor and R. Soydaner-Azeloglu for discussions and help with manuscript preparation, J.S. Handler and E. Bekes for technical assistance, and the members of the Bar-Sagi laboratory for comments. The FACS, Histopathology Cores, and Tissue Acquisition and Biorepository Service of NYU School of Medicine are partially supported by the National Institutes of Health (Grant 5 P30CA016087-31). This work was supported by the National Institutes of Health (Grant CA055360) and AACR-PanCAN (Grant 08-60-25-BARS) (both to D.B.-S.) and by The Irvington Institute Postdoctoral Fellowship Program of the Cancer Research Institute (support to Y.P.-G.).

Received: July 13, 2011
Revised: February 5, 2012
Accepted: April 9, 2012
Published: June 11, 2012

REFERENCES

Agbunag, C., Lee, K.E., Buontempo, S., and Bar-Sagi, D. (2006). Pancreatic duct epithelial cell isolation and cultivation in two-dimensional and three-dimensional culture systems. Methods Enzymol. *407*, 703–710.

Ancrile, B.B., O'Hayer, K.M., and Counter, C.M. (2008). Oncogenic ras-induced expression of cytokines: a new target of anti-cancer therapeutics. Mol. Interv. *8*, 22–27.

Barreda, D.R., Hanington, P.C., and Belosevic, M. (2004). Regulation of myeloid development and function by colony stimulating factors. Dev. Comp. Immunol. *28*, 509–554.

Bronte, V., Chappell, D.B., Apolloni, E., Cabrelle, A., Wang, M., Hwu, P., and Restifo, N.P. (1999). Unopposed production of granulocyte-macrophage colony-stimulating factor by tumors inhibits CD8+ T cell responses by dysregulating antigen-presenting cell maturation. J. Immunol. *162*, 5728–5737.

Bunt, S.K., Yang, L., Sinha, P., Clements, V.K., Leips, J., and Ostrand-Rosenberg, S. (2007). Reduced inflammation in the tumor microenvironment delays the accumulation of myeloid-derived suppressor cells and limits tumor progression. Cancer Res. *67*, 10019–10026.

Carragher, D.M., Rangel-Moreno, J., and Randall, T.D. (2008). Ectopic lymphoid tissues and local immunity. Semin. Immunol. *20*, 26–42.

Chu, G.C., Kimmelman, A.C., Hezel, A.F., and DePinho, R.A. (2007). Stromal biology of pancreatic cancer. J. Cell. Biochem. *101*, 887–907.

Clark, C.E., Hingorani, S.R., Mick, R., Combs, C., Tuveson, D.A., and Vonderheide, R.H. (2007). Dynamics of the immune reaction to pancreatic cancer from inception to invasion. Cancer Res. *67*, 9518–9527.

Clark, C.E., Beatty, G.L., and Vonderheide, R.H. (2009). Immunosurveillance of pancreatic adenocarcinoma: insights from genetically engineered mouse models of cancer. Cancer Lett. *279*, 1–7.

Coppé, J.P., Patil, C.K., Rodier, F., Sun, Y., Muñoz, D.P., Goldstein, J., Nelson, P.S., Desprez, P.Y., and Campisi, J. (2008). Senescence-associated secretory phenotypes reveal cell-nonautonomous functions of oncogenic RAS and the p53 tumor suppressor. PLoS Biol. *6*, 2853–2868.

Dolcetti, L., Peranzoni, E., Ugel, S., Marigo, I., Fernandez Gomez, A., Mesa, C., Geilich, M., Winkels, G., Traggiai, E., Casati, A., et al. (2010). Hierarchy of immunosuppressive strength among myeloid-derived suppressor cell subsets is determined by GM-CSF. Eur. J. Immunol. *40*, 22–35.

DuPage, M., Cheung, A.F., Mazumdar, C., Winslow, M.M., Bronson, R., Schmidt, L.M., Crowley, D., Chen, J., and Jacks, T. (2011). Endogenous T cell responses to antigens expressed in lung adenocarcinomas delay malignant tumor progression. Cancer Cell *19*, 72–85.

Fossum, B., Olsen, A.C., Thorsby, E., and Gaudernack, G. (1995). CD8+ T cells from a patient with colon carcinoma, specific for a mutant p21-Ras-derived

peptide (Gly13→Asp), are cytotoxic towards a carcinoma cell line harbouring the same mutation. Cancer Immunol. Immunother. *40*, 165–172.

Fukuda, A., Wang, S.C., Morris, J.P., 4th, Folias, A.E., Liou, A., Kim, G.E., Akira, S., Boucher, K.M., Firpo, M.A., Mulvihill, S.J., and Hebrok, M. (2011). Stat3 and MMP7 contribute to pancreatic ductal adenocarcinoma initiation and progression. Cancer Cell *19*, 441–455.

Gabrilovich, D.I., and Nagaraj, S. (2009). Myeloid-derived suppressor cells as regulators of the immune system. Nat. Rev. Immunol. *9*, 162–174.

Gedde-Dahl, T., 3rd, Spurkland, A., Fossum, B., Wittinghofer, A., Thorsby, E., and Gaudernack, G. (1994). T cell epitopes encompassing the mutational hot spot position 61 of p21 ras: promiscuity in ras peptide binding to HLA. Eur. J. Immunol. *24*, 410–414.

Gjertsen, M.K., and Gaudernack, G. (1998). Mutated Ras peptides as vaccines in immunotherapy of cancer. Vox Sang. *74* (*Suppl 2*), 489–495.

Grivennikov, S.I., Greten, F.R., and Karin, M. (2010). Immunity, inflammation, and cancer. Cell *140*, 883–899.

Hamilton, J.A. (2008). Colony-stimulating factors in inflammation and autoimmunity. Nat. Rev. Immunol. *8*, 533–544.

Hingorani, S.R., Petricoin, E.F., Maitra, A., Rajapakse, V., King, C., Jacobetz, M.A., Ross, S., Conrads, T.P., Veenstra, T.D., Hitt, B.A., et al. (2003). Preinvasive and invasive ductal pancreatic cancer and its early detection in the mouse. Cancer Cell *4*, 437–450.

Hingorani, S.R., Wang, L., Multani, A.S., Combs, C., Deramaudt, T.B., Hruban, R.H., Rustgi, A.K., Chang, S., and Tuveson, D.A. (2005). Trp53R172H and KrasG12D cooperate to promote chromosomal instability and widely metastatic pancreatic ductal adenocarcinoma in mice. Cancer Cell *7*, 469–483.

Hong, S.M., Park, J.Y., Hruban, R.H., and Goggins, M. (2011). Molecular signatures of pancreatic cancer. Arch. Pathol. Lab. Med. *135*, 716–727.

Jackson, E.L., Willis, N., Mercer, K., Bronson, R.T., Crowley, D., Montoya, R., Jacks, T., and Tuveson, D.A. (2001). Analysis of lung tumor initiation and progression using conditional expression of oncogenic K-ras. Genes Dev. *15*, 3243–3248.

Kawaguchi, Y., Cooper, B., Gannon, M., Ray, M., MacDonald, R.J., and Wright, C.V. (2002). The role of the transcriptional regulator Ptf1a in converting intestinal to pancreatic progenitors. Nat. Genet. *32*, 128–134.

Kern, S.E., Shi, C., and Hruban, R.H. (2011). The complexity of pancreatic ductal cancers and multidimensional strategies for therapeutic targeting. J. Pathol. *223*, 295–306.

Kleeff, J., Beckhove, P., Esposito, I., Herzig, S., Huber, P.E., Lohr, J.M., and Friess, H. (2007). Pancreatic cancer microenvironment. Int. J. Cancer *121*, 699–705.

Kranenburg, O., Gebbink, M.F., and Voest, E.E. (2004). Stimulation of angiogenesis by Ras proteins. Biochim. Biophys. Acta *1654*, 23–37.

Kubuschok, B., Neumann, F., Breit, R., Sester, M., Schormann, C., Wagner, C., Sester, U., Hartmann, F., Wagner, M., Remberger, K., et al. (2006). Naturally occurring T-cell response against mutated p21 ras oncoprotein in pancreatic cancer. Clin. Cancer Res. *12*, 1365–1372.

Lee, K.E., and Bar-Sagi, D. (2010). Oncogenic KRas suppresses inflammation-associated senescence of pancreatic ductal cells. Cancer Cell *18*, 448–458.

Lesina, M., Kurkowski, M.U., Ludes, K., Rose-John, S., Treiber, M., Klöppel, G., Yoshimura, A., Reindl, W., Sipos, B., Akira, S., et al. (2011). Stat3/Socs3 activation by IL-6 transsignaling promotes progression of pancreatic intraepithelial neoplasia and development of pancreatic cancer. Cancer Cell *19*, 456–469.

Linard, B., Bézieau, S., Benlalam, H., Labarrière, N., Guilloux, Y., Diez, E., and Jotereau, F. (2002). A ras-mutated peptide targeted by CTL infiltrating a human melanoma lesion. J. Immunol. *168*, 4802–4808.

Maitra, A., and Hruban, R.H. (2008). Pancreatic cancer. Annu. Rev. Pathol. *3*, 157–188.

Marigo, I., Dolcetti, L., Serafini, P., Zanovello, P., and Bronte, V. (2008). Tumor-induced tolerance and immune suppression by myeloid derived suppressor cells. Immunol. Rev. *222*, 162–179.

Marigo, I., Bosio, E., Solito, S., Mesa, C., Fernandez, A., Dolcetti, L., Ugel, S., Sonda, N., Bicciato, S., Falisi, E., et al. (2010). Tumor-induced tolerance and immune suppression depend on the C/EBPbeta transcription factor. Immunity *32*, 790–802.

Melani, C., Chiodoni, C., Forni, G., and Colombo, M.P. (2003). Myeloid cell expansion elicited by the progression of spontaneous mammary carcinomas in c-erbB-2 transgenic BALB/c mice suppresses immune reactivity. Blood *102*, 2138–2145.

Morales, J.K., Kmieciak, M., Knutson, K.L., Bear, H.D., and Manjili, M.H. (2010). GM-CSF is one of the main breast tumor-derived soluble factors involved in the differentiation of CD11b-Gr1- bone marrow progenitor cells into myeloid-derived suppressor cells. Breast Cancer Res. Treat. *123*, 39–49.

Mroczko, B., Szmitkowski, M., Wereszczyńska-Siemiatkowska, U., and Jurkowska, G. (2005). Hematopoietic cytokines in the sera of patients with pancreatic cancer. Clin. Chem. Lab. Med. *43*, 146–150.

Osborne, C.S., Vadas, M.A., and Cockerill, P.N. (1995). Transcriptional regulation of mouse granulocyte-macrophage colony-stimulating factor/IL-3 locus. J. Immunol. *155*, 226–235.

Ostrand-Rosenberg, S., and Sinha, P. (2009). Myeloid-derived suppressor cells: linking inflammation and cancer. J. Immunol. *182*, 4499–4506.

Pilon-Thomas, S., Nelson, N., Vohra, N., Jerald, M., Pendleton, L., Szekeres, K., and Ghansah, T. (2011). Murine pancreatic adenocarcinoma dampens SHIP-1 expression and alters MDSC homeostasis and function. PLoS ONE *6*, e27729.

Pylayeva-Gupta, Y., Grabocka, E., and Bar-Sagi, D. (2011). RAS oncogenes: weaving a tumorigenic web. Nat. Rev. Cancer *11*, 761–774.

Qin, H., Chen, W., Takahashi, M., Disis, M.L., Byrd, D.R., McCahill, L., Bertram, K.A., Fenton, R.G., Peace, D.J., and Cheever, M.A. (1995). CD4+ T-cell immunity to mutated ras protein in pancreatic and colon cancer patients. Cancer Res. *55*, 2984–2987.

Quezada, S.A., Peggs, K.S., Simpson, T.R., and Allison, J.P. (2011). Shifting the equilibrium in cancer immunoediting: from tumor tolerance to eradication. Immunol. Rev. *241*, 104–118.

Ruffell, B., DeNardo, D.G., Affara, N.I., and Coussens, L.M. (2010). Lymphocytes in cancer development: polarization towards pro-tumor immunity. Cytokine Growth Factor Rev. *21*, 3–10.

Schön, M., Denzer, D., Kubitza, R.C., Ruzicka, T., and Schön, M.P. (2000). Critical role of neutrophils for the generation of psoriasiform skin lesions in flaky skin mice. J. Invest. Dermatol. *114*, 976–983.

Seidler, B., Schmidt, A., Mayr, U., Nakhai, H., Schmid, R.M., Schneider, G., and Saur, D. (2008). A Cre-loxP-based mouse model for conditional somatic gene expression and knockdown in vivo by using avian retroviral vectors. Proc. Natl. Acad. Sci. USA *105*, 10137–10142.

Shi, C., Fukushima, N., Abe, T., Bian, Y., Hua, L., Wendelburg, B.J., Yeo, C.J., Hruban, R.H., Goggins, M.G., and Eshleman, J.R. (2008). Sensitive and quantitative detection of KRAS2 gene mutations in pancreatic duct juice differentiates patients with pancreatic cancer from chronic pancreatitis, potential for early detection. Cancer Biol. Ther. *7*, 353–360.

Steube, K.G., Meyer, C., and Drexler, H.G. (1998). Secretion of functional hematopoietic growth factors by human carcinoma cell lines. Int. J. Cancer *78*, 120–124.

Tu, S., Bhagat, G., Cui, G., Takaishi, S., Kurt-Jones, E.A., Rickman, B., Betz, K.S., Penz-Oesterreicher, M., Bjorkdahl, O., Fox, J.G., and Wang, T.C. (2008). Overexpression of interleukin-1beta induces gastric inflammation and cancer and mobilizes myeloid-derived suppressor cells in mice. Cancer Cell *14*, 408–419.

Weijzen, S., Velders, M.P., and Kast, W.M. (1999). Modulation of the immune response and tumor growth by activated Ras. Leukemia *13*, 502–513.